A theoretical STM study of Co_n/Pt(111)

Peter Weinberger

A theoretical STM study of Co_{n}/Pt(111)

Journal:	*Philosophical Magazine & Philosophical Magazine Letters*
Manuscript ID:	TPHM-10-Oct-0439.R1
Journal Selection:	Philosophical Magazine
Date Submitted by the Author:	24-Nov-2010
Complete List of Authors:	Weinberger, Peter; Center for Computational Nanoscience
Keywords:	magnetism, magnetization dynamics, STM
Keywords (user supplied):	

A theoretical STM study of $Co_n/Pt(111)$

P. Weinberger[1]

[1] *Center for Computational Nanoscience, Seilerstätte 10/22, A 1010 Vienna, Austria*

It is shown that by "stacking" together a semi-infinite sample subsystem with a semi-infinite tip subsystem difficulties with respect to a common Fermi level for the whole system can approximately be overcome in all those cases when the substrate (serving as lead) and the second lead are different materials. Based on this procedure by means of the spin-polarized (fully) relativistic Screened Korringa-Kohn-Rostocker method and an equivalent Kubo equation theoretical spin-polarized STM spectra for $Pt(111)/Co_n/Cr_{15}W_{22}/Cu(111)$ with respect to an applied external magnetic field are evaluated in terms of difference conductivities as a function of the corresponding free energy. These spectra are interpreted using layer-resolved contributions to the difference conductivities in order to indicate which parts of the sample dominate changes in the tunneling current caused by changing the orientation of the magnetization. Also shown are estimates of the time scales to switch from perpendicular to in-plane and vice versa. All investigated properties suggest that different situations apply when the number of Co layers on top of Pt(111) is increased from one to three.

INTRODUCTION

In the last few years the number of publications devoted to spin-polarized scanning tunnel microscopy (STM) increased substantially, see the impressive review article by Wiesendanger [1] and in particular Refs. [2] - [5], claiming that by now the magnetic switching properties of single atoms or at least of very small islands of magnetic atoms can be determined experimentally. Now-a-days even the use of external surprisingly high magnetic vector fields became possible, the lateral precision in moving the tip having been reduced already to a fraction of the spacial extension of an atom on top of a surface. The experimentally investigated samples usually consist of an ensemble of magnetic atoms or a few monolayers of a magnetic material placed on a suitable substrate such as for example Cu(111) or Pt(111). Very often a so-called Cr/W-tip prepared with about 10 layers of Cr and a thick slab of W is used. This tip is connected in turn to a lead. The width of the vacuum barrier between the sample and the tip is typically below 10Å. The substrate and the lead on top of the tip carry the necessary electric contacts for the measurements. Quite clearly, since the tunneling current is a non-local quantity, in order to describe STM spectra theoretically the whole system consisting of the substrate (serving as a lead), the magnetic adsorbate, the tip and the second lead ought to be taken into account.

Based on Bardeen's suggestion [6] STM experiments are usually interpreted theoretically in terms of the so-called Tersoff-Hamann approach [7, 8] in which the tunneling current is replaced by the charge density corresponding to the surface local density of states. Frequently also approximations to Bardeen's matrix element are included, which, however, in its original form is very difficult to evaluate since it combines nonorthogonal eigenstates of different Hamiltonians, namely those "of the probe" and "of the surface". These approximations are mostly based on spherically shaped tips [7, 8] and on using an s-wave for the tip wave function. In the past the Tersoff-Hamann approach proved to be extremely successful in interpreting experimental data, see, e.g. Ref. [9] and in particular Refs. [10] - [12].

With the arrival of spin-polarized STM techniques, however, different theoretical approaches were needed, since it was quickly realized that for non-collinear magnetic structures (at least) spin-orbit interactions had to be included [13, 14]. Unfortunately, in using a Tersoff-Hamann approach even on an appropriate spin-polarized *ab initio* level, the difficulties with Bardeen's matrix elements remain, and, in particular, one of the main features of modern experimental techniques, namely of applying an external magnetic field, cannot be described properly.

Because of the non-locality of the tunneling current it was and partially still is a matter of belief to claim that STM is an "atomic"- or "surface" specific experimental tool, whereby even the term "surface" is a bit misleading, since also buried magnetic structures can be "seen" in STM. In order to shed some light on the question of what actually is "seen" in a spin-polarized STM experiment and also to overcome the limitations of the Tersoff-Hamann approach it was suggested [15, 16] to directly calculate the tunneling current in terms of a Kubo equation based on (fully) relativistic scattering theory, i.e., based on the Dirac equation, which of course describes spin-orbit interactions correct to all orders of the speed of light. By displaying (difference) conductivities as functions of the anisotropy energy, which in turn is proportional to the applied external magnetic field, it was shown that experimentally observed di/dV curves with respect to an applied magnetic field can be reasonably well reproduced. In particular layer-resolved differences in conductivities as functions of the anisotropy energy turned out to be a useful tool to point out which parts of the whole system contribute most to the total difference in conductivities.

Up to now this approach was only applied to systems in which the substrate and the lead on top of the tip are

the same material [15, 16], which of course determines the Fermi level. If, however, the substrate (semi-infinite system carrying one contact) on which magnetic atoms or islands are deposited is different from the material (lead, semi-infinite system) connecting the tip to the other contact, then approximations to the condition of a common Fermi level have to be made. Clearly, although magnetic islands can be viewed as nanosystems, the whole system is of course macro-sized, the substrate as well as the lead on top of the tip serving in principle as electron reservoirs for any kind of electric transport properties.

The easy way out, namely discarding the tip subsystem from a description of the electric properties of such a system, leads to a completely wrong model of electric transport, since a semi-infinite vacuum barrier only creates reflecting boundary conditions.[17] This, simply speaking, means that no second contact can be "welded" on: without a second contact, however, no measurements of electric properties can be made and therefore also no STM experiments.

If therefore two semi-infinite systems of different material separated by a vacuum barrier have to be taken into account, formally the same difficulties as in Bardeen's orginal model and in the Tersoff-Hamann approach arise when using Density Functional Theory, namely the necessity to deal with two Green's functions (Hamiltonians) of different spectral properties. An approximate way to deal with this situation is discussed in the following section.

Furthermore, beyond the problem of two leads of different type the geometrical shape of the two subsystems that are linked together via a vacuum barrier ought to be taken into account. Since parts of both subsystems are nano-sized in two dimensions [18] and therefore no longer are two-dimensional translationally invariant, in principle one ought to use a real space description not only for the electronic and magnetic properties of the total system but also for the electric transport properties. Although in principle this can be achieved by using, e.g., the so-called Embedded Cluster Method (ECM) [18, 19] and a real space scattering version of the Kubo equation [20] the computational effort to be encountered is quite substantial and therefore most likely is not suitable for routine-like investigations.

Clearly, by approximating such a real space description by one based on two-dimensional translational symmetry, implying in turn that only "flat tips" and completely decorated atomic layers are considered, no longer particular shapes of the tip can be taken into account and also "atom-like" features of the tunneling current cannot be reproduced. However, in terms of such an approximation systems reflecting realistic thickness parameters can be investigated on a computationally surmountable level. For this very reason in here use is made of the computational simplifications provided by two-dimensional translational symmetry.

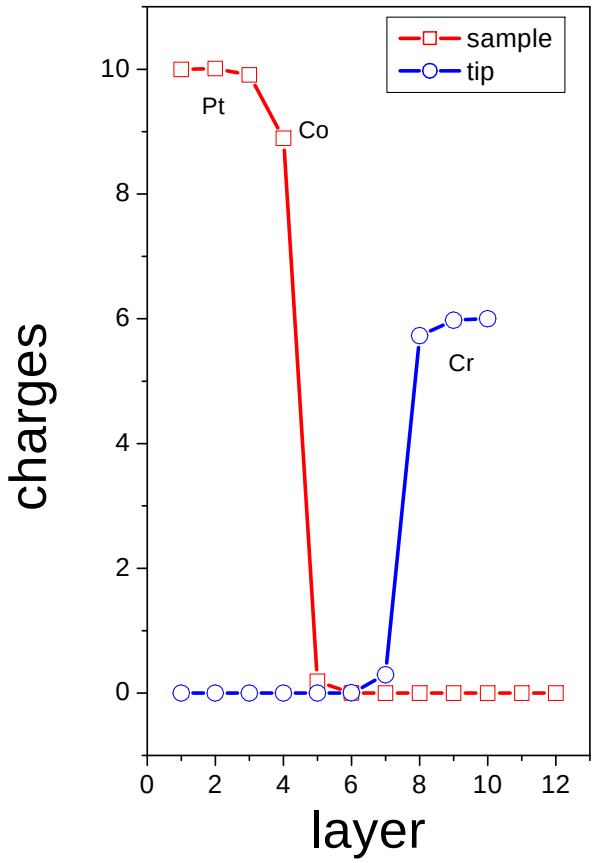

FIG. 1: (color online) "Stacking together" systems I and II. Shown are the charges/layer in the vicinity of the vacuum barrier.

Finally, one has to realize that with all reorientations of the magnetization enforced by an external magnetic field a particular dynamics is connected, implying, e.g., that certain parts of an experimental STM spectrum (di/dV versus applied magnetic field) correspond to fast reorientations of the magnetization and others to slower processes. For this reason also estimates of the switching times are presented as based on the Landau-Lifshitz-Gilbert equation by using internal fields calculated on an ab-initio level.

Clearly, a theoretical description of experimental di/dV curves with respect to the applied sample bias (voltage) is even more complicated, since then also current-induced changes in the orientation of the magnetization have to be taken into account. Up-to-now only a formal discussion of how to deal with this problem in the presence of spin-orbit coupling was presented. [21]

In the following sections first the construction of the applied scattering potentials is described, then the evaluation of the hypersurfaces of the free energy and of difference conductivities (contrast, di/dV) is discussed, includ-

ing a formal scheme of interpretation of these difference conductivities and an estimate for the dynamics involved. Only then the ultimate goal of the present investigations is achieved, namely displaying theoretical STM spectra in terms of difference conductivities (contrast) versus free energy (applied external magnetic field), i.e., obtaining curves that directly can be compared to experimental di/dV data when applying an external magnetic field.

STACKING SYSTEMS

Consider for example the system Pt(111)/Co$_n$, i.e., a Pt(111) surface covered by n complete overlayers of Co. The magnetic properties (spin and orbital moments, magnetic anisotropy energy) of a free surface of Co adlayers or of Co clusters on Pt(111) were already studied extensively in the past [22–24]. However, viewed as sample system in an STM experiment, the situation becomes less straight forward, since as already was mentioned a tip with a lead has to be included. In using for example a typical Cr/W tip one obviously is faced with the problem to deal theoretically with a system of the following kind,

$$\underbrace{\mathrm{Pt(111)}}_{\text{semi-finite}}/\mathrm{Pt}_m\mathrm{Co}_n\mathrm{Vac}_3\underbrace{\mathrm{Cr}_{15}\mathrm{W}_{22}}_{\text{tip}}\mathrm{Cu}_t/\underbrace{\text{Cu-lead}}_{\text{semi-finite}} \quad (1)$$

in which the thickness parameters are given in terms of monolayers. Fortunately, because of the vacuum barrier the sample subsystem is only very weakly coupled to the tip subsystem. It is therefore tempting to first calculate selfconsistently both subsystem as free surfaces,

$$\underbrace{\mathrm{Pt(111)}/\mathrm{Pt}_m\mathrm{Co}_n\mathrm{Vac}_r}_{\text{free surface I}}\ ,\ \underbrace{\mathrm{Vac}_s\mathrm{Cr}_{15}\mathrm{W}_{22}\mathrm{Cu}_t/\mathrm{Cu(111)}}_{\text{free surface II}} \quad (2)$$

$$m \geq 12,\ r,s \geq 3,\ t \geq 15$$

for an illustration see Fig. 1, and then "stack" them together in the following manner

$$\underbrace{\mathrm{Pt(111)}/\mathrm{Pt}_m\mathrm{Co}_n\mathrm{Vac}_2}_{\text{I: sample subsystem, }\Theta_1}\ /\ \underbrace{\mathrm{Vac}_1\mathrm{Cr}_{15}\mathrm{W}_{22}\mathrm{Cu}_t/\mathrm{Cu(111)}}_{\text{II: tip subsystem, }\Theta_2} \quad (3)$$

Independent calculations for free surfaces imply that, disregarding possible relaxation effects in the surface-near region, for the sample subsystem the lattice spacing and Fermi energy of bulk fcc Pt has to be used, while for the tip subsystem the corresponding quantities for fcc Cu apply. In terms of charges in the vacuum barrier the error to be encountered by such a stacking procedure is of the order of a few thousandth of an electron. For example, treating the subsystems of the system listed in (2) as free surfaces one finds that the charge in the second vacuum layer of Pt(111)/Pt$_m$Co$_n$Vac$_r$ amounts to 0.00115 electrons, while for Vac$_s$Cr$_{15}$W$_{22}$Cu$_t$/Cu(111) the corresponding charge is 0.00556 electrons. Clearly, for $r, s > 2$ the corresponding charges are substantially less.

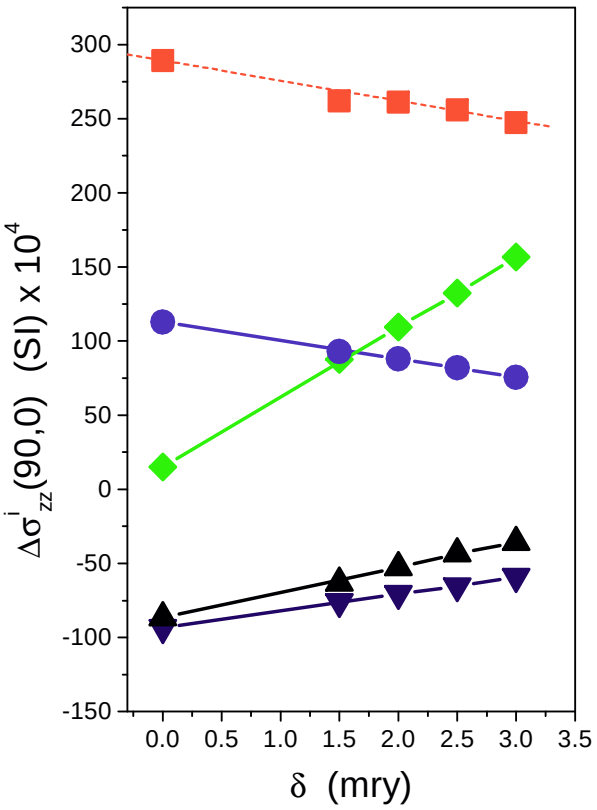

FIG. 2: (color online) Numerical continuation of local difference conductivities $\Delta\sigma^i_{zz}(\Theta_1, 0)$, $\Theta_1 = 90$, $\Theta_1^{(r)}, \Theta_2^{(r)} = 0$, see Eq. (9), to the real axis for Pt(111) covered by a single layer of Co. Diamonds denote the Co layer, squares, up- and down triangles in turn the first, second and third Pt layer beneath, circles refer to the first vacuum layer ("surface state").

To consider as indicated in (3) the selfconsistent scattering potentials of the two subsystems as a single set of such scattering potentials to be used for an evaluation of electric properties in terms of the Kubo equation and of the free energy has to be regarded as a simple approximation for the joining up of two Green's functions of different spectral properties to a single one for the whole system; as an attempt to cope with spin-polarized STM experiments in which the two leads are of different matter.

FREE ENERGIES

Based on the assumption that the tip system is supposed to add little to the free energy (at zero temperature

system	$\Delta E(90,0)$ (meV)
$Pt(111)/Pt_{12}Co_1Vac_6$ [24]	0.091
$Pt(111)/Pt_{12}Co_1Vac_3$	
$Cr_{15}W_{22}Cu_{15}/Cu(111)$	0.092

TABLE I: Comparison of the reorientation energy $\Delta E(90,0)$ for a free surface of a single ML of Co on Pt(111) and in the stacked together system.

[19]) of the system in (3),

$$\Delta E(\Theta_1,\Theta_2) = E(\Theta_1,\Theta_2) - E(\Theta_1^{(r)},\Theta_2^{(r)}) \quad (4)$$

$$= \sum_{i=1,N} \Delta E^i(\Theta_1,\Theta_2) \ , \quad (5)$$

it seems to be quite reasonable to use the Fermi energy and lattice spacing of the substrate, namely Pt(111) for the combined system in (1). In Eq. (4), as indicated in (3), Θ_1 and Θ_2 specify uniform orientations of the magnetization in the sample (Θ_1) and in the tip part (Θ_2) confined to the xz-plane, x being the in-plane x-axis and z the surface normal: Θ_1 and Θ_2 are rotation angles around the respective in-plane y-axes; $\Theta_1^{(r)}$ and $\Theta_2^{(r)}$ specify given reference orientations. The $\Delta E^i(\Theta_1,\Theta_2)$ in Eq. (5) are the so-called layer-resolved free energies, $N = m+n+t+40$. The comparison in Table I shows that the approximations made up to now are indeed quite reasonable: the reorientation energy $\Delta E(90,0)$, $\Theta_1^{(r)},\Theta_2^{(r)} = 0$, for the system in (3) differs only little from that for a free surface of a single Co layer on top of Pt(111).

DIFFERENCE CONDUCTIVITIES

For given values of Θ_1 and Θ_2 the current perpendicular to the planes of atoms is given [26–33] for the system in (1) by

$$j_z(\Theta_1,\Theta_2) = \sum_{i=1,N} j_z^i(\Theta_1,\Theta_2) = \sum_{j=1,N} \sigma_{zz}^{ij}(\Theta_1,\Theta_2)\mathcal{E}_z^j \ , \quad (6)$$

$$j_z^i(\Theta_1,\Theta_2) \sim \mathcal{E} \sum_{j=1,N} \sigma_{zz}^{ij}(\Theta_1,\Theta_2) = \mathcal{E}\sigma_{zz}^{i}(\Theta_1,\Theta_2) \ , \quad (7)$$

where the $\sigma_{zz}^{ij}(\Theta_1,\Theta_2)$ are layer-wise contributions to the zz-element of the conductivity tensor and $\mathcal{E}_z^j$ is the z-component of the electric field in atomic layer j. As indicated in Eq. (7) $j_z(\Theta_1,\Theta_2)$ can **formally** be decomposed [25] into layer-resolved contributions $j_z^i(\Theta_1,\Theta_2)$, keeping in mind, however, that only the total current $j_z(\Theta_1,\Theta_2)$ is well defined!

Since usually not the current *per se* is of interest but rather the difference with respect to a given reference configuration $\Theta_1^{(r)}$ and $\Theta_2^{(r)}$, it is useful [15, 16] to define the following quantities,

$$\Delta j_z(\Theta_1,\Theta_2) = \sum_{i=1}^{N} \Delta j_z^i(\Theta_1,\Theta_2) \sim \mathcal{E}\sum_{i=1}^{N} \Delta\sigma_{zz}^{i}(\Theta_1,\Theta_2) \ , \quad (8)$$

$$\Delta\sigma_{zz}^{i}(\Theta_1,\Theta_2) = \sum_{j=1}^{N} \left(\sigma_{zz}^{ij}(\Theta_1,\Theta_2) - \sigma_{zz}^{ij}(\Theta_1^{(r)},\Theta_2^{(r)})\right)$$

$$= \Delta\sigma_{zz}^{ii}(\Theta_1,\Theta_2) + \Delta\bar{\sigma}_{zz}^{i}(\Theta_1,\Theta_2) \ , \quad (9)$$

$$\Delta\bar{\sigma}_{zz}^{i}(\Theta_1,\Theta_2) = \sum_{j=1}^{N} \Delta\sigma_{zz}^{ij}(\Theta_1,\Theta_2)(1-\delta_{ij}) \ . \quad (10)$$

It is important to note that as the angles Θ_1 and Θ_2 vary $\Delta\sigma_{zz}(\Theta_1,\Theta_2)$ is supposed to map the change in "contrast" to be seen in experiment as the orientation of the external magnetic field is changed.

In using, e.g., $\Theta_1 = 90, \Theta_2 = 0$ and $\Theta_1^{(r)},\Theta_2^{(r)} = 0$, $\Delta\sigma_{zz}(\Theta_1,\Theta_2)$ corresponds to the difference in the zz-like conductivity between a perpendicular and an in-plane orientation of the magnetization in the sample subsystem only, whereas for $\Theta_1,\Theta_2 = 90$ and $\Theta_1^{(r)},\Theta_2^{(r)} = 0$ the orientation of the magnetization in both the sample and the tip changes from perpendicular to in-plane.

COMPUTATIONAL APPROACH

All *ab initio* electronic structure calculations were performed for a uniform direction of the magnetization pointing along the surface normal in terms of the spin-polarized (fully) relativistic screened Korringa-Kohn-Rostoker method.[19] The band energies in Eq. (4) are evaluated (at zero temperature) in terms of the magnetic force theorem [18] by integrating in the upper half of the complex energy plane along a contour starting at E_0 and ending at the Fermi energy. The electric transport properties were evaluated by means of the fully relativistic Kubo-Greenwood equation,[18, 19] by making use of complex Fermi energies $\mathcal{E}_F = E_F + i\delta$ and subsequent numerical continuation to the real energy axis. Finally, the Landau-Lifshitz-Gilbert equation was solved using the approach and the approximations discussed in Ref. [38]. In all calculations a maximum angular quantum number of two,[19] the density functional parametrization of Ref. [39] and the atomic sphere approximation (ASA) were used.

Quite clearly the procedure suggested, namely to separately evaluate selfconsistently the subsystems as free surfaces, the stacking of the subsystems and the choice of the Fermi energy to be that of the substrate only results from the need to specify a common Fermi energy. The need to have only one in-plane lattice spacing arises from the fact that in order to make use of Brillouin zone integrations one and the same two-dimensional translational symmetry has to apply in all layers of the system.

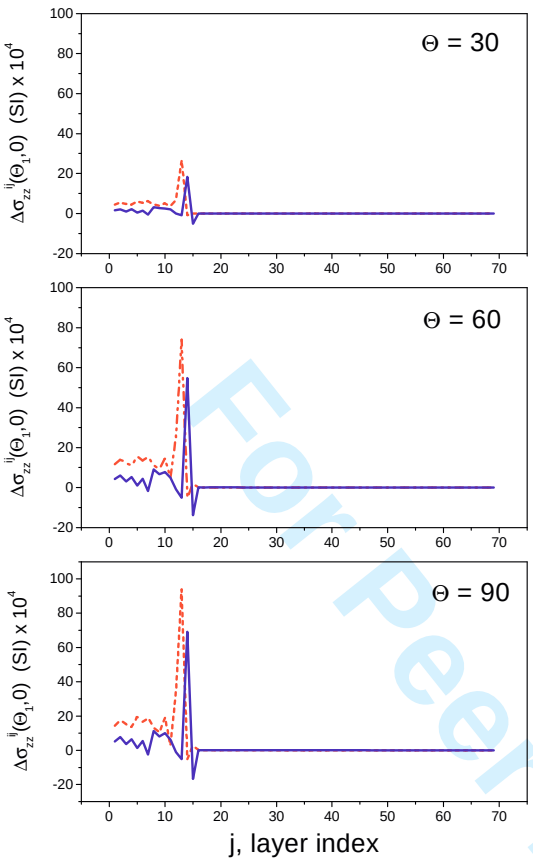

FIG. 3: (color online) Evolution of peaks in the layer-wise contributions, $\Delta\sigma_{zz}^{ij}(\Theta,0)$, $\Theta_1^{(r)},\Theta_2^{(r)}=0$, to the total difference conductivity for Pt(111)/Co when varying Θ between 0 and 90. Note that $\Delta\sigma_{zz}^{ij}(0,0)$ is of course zero for all i and j. The full line applies when i refers to the Co layer, the dashed line to the Pt layer beneath.

Variations in the interlayer distances, however, can be taken into account either directly [19] or approximately [40]. Of course in a real space description no restrictions caused by translational symmetry apply, however, then the size of the clusters considered matters quite a bit.

Continuation to the real energy axis

It is worthwhile to illustrate at least once the numerical continuation to the real energy axis mentioned above, in particular, since a surprising feature can be discovered. In Fig. 2 this continuation is displayed for the Co layer as well as for the first three Pt layers beneath and the first vacuum layer in Pt(111)/Co. It was shown by Palotas *et. al.* [41] by using a real space Kubo formulation that the zz-like element of the conductivity tensor at complex energies $(E_F, i\delta)$ is linear in δ. As can be seen from Fig. 2 the dependence of the layer-wise contributions to the total difference conductivity on the imaginary part of the Fermi energy is strictly linear with the exception for the top Pt layer for which a numerical error of less than about 5% applies.

Obviously in this figure all layer-wise contributions but the one for the first vacuum layer do have negative slopes with respect to δ. In order to interpret the behavior of this vacuum layer one has to remember that a finite δ acts like an additional selfenergy. If metallic electric transport applies then with increasing δ the conductivity increases because of increased selfenergy. If, however, tunneling or non-metallic transport is present then with increasing δ the conductivity decreases. [33] Viewed in this way Fig. 2 indicates that in this layer a tunneling-type of electric transport occurs.

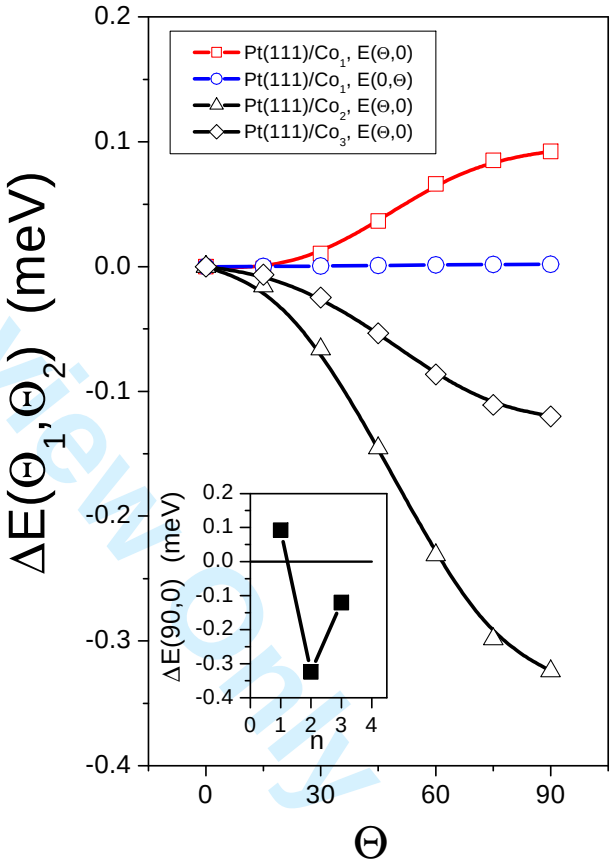

FIG. 4: (color online) Free energy $\Delta E(\Theta_1,\Theta_2)$, $\Theta_1^{(r)},\Theta_2^{(r)}=0$, corresponding to $n\leq 3$ monolayers of Co on top of Pt(111). In the case of a single monolayer of Co also the free energy corresponding to the tip part of the system is displayed. The inset shows the reorientation (from perpendicular to in-plane) energy as a function of n.

Meaning of layer-wise contributions to the total difference conductivity

The physical meaning of the layer-wise contributions to the total difference conductivity can best be seen by viewing these quantities in the two-dimensional space spanned by the layer indices i and j. In Fig. 3 two cases are depicted, namely when i refers either to the Co or the first Pt layer beneath and j varies over all other atomic layers in Pt(111)/Co/tip/Cu(111). Shown is the variation with Θ_1. As can be seen there is a large peak evolving exactly when $i = j$. Quite obviously, $\Delta\sigma^i_{zz}(\Theta_1, 0) \sim \Delta\sigma^{ii}_{zz}(\Theta_1, 0)$, since in Eq. (9) $\Delta\sigma^{ii}_{zz}(\Theta_1, 0) \gg \Delta\bar{\sigma}^i_{zz}(\Theta_1, 0)$.[42] It should be noted that the peaks in Fig. 3 only grow when increasing Θ_1. Of course for $\Theta_1 = 0$ there is no such peak!

The layer-wise resolved contributions to the total difference conductivity have to be viewed as a qualitative tool of interpretation to trace locally the effect of changes in the orientation of the magnetization. It is important, however, to recall – as already said – that only the total difference conductivity $\Delta\sigma_{zz}(\Theta_1, \Theta_2)$ is well-defined, namely as the sum over all layer-wise contributions $\Delta\sigma^i_{zz}(\Theta_1, \Theta_2)$, since per definition a current is a non-local quantity.

PT(111)/CO$_n$

Free energies and difference conductivities

In Fig. 4 the free energies $\Delta E(\Theta_1, 0)$ for Pt(111)/Pt$_m$Co$_n$Vac$_3$Cr$_{15}$W$_{22}$Cu$_{15}$/Cu(111), $m \geq 12, n \leq 3$, are displayed versus Θ_1 together with $\Delta E(0, \Theta_2)$ for $n = 1$ as a function of Θ_2. As can be seen for $n = 1$ the free energy prefers a perpendicular orientation of the magnetization, while for $n \geq 2$ an in-plane orientation of the magnetization is present. As can be seen from this figure, the tip indeed adds only a small positive contribution to the free energy.

In the top parts of Figs. 5 - 7 the layer-wise contributions to the total difference conductivity $\Delta\sigma^i_{zz}(90, 0), i = 1, N$, are displayed, while in the bottom parts of these figures the $\Delta\sigma^i_{zz}(\Theta_1, 0)$ corresponding to atomic layers in the vicinity of the Pt/Co/Vac interface are shown as functions of Θ_1. It is perhaps surprising to realize (Fig. 5) that in the case of a single layer of Co on Pt(111) the main contribution to the difference conductivity is not due to the Co layer but due to the Pt layer immediately beneath the surface and that the first vacuum layer ("surface state") adds very little to $\Delta\sigma_{zz}(\Theta_1, 0)$. For $n = 2$, see Fig. 6, the situation is completely different: now the two Co layers and the first Pt layer contribute most to the total difference conductivity as one would intuitively expect. For $n = 3$, see Fig. 7, the contribution from the most interior Co layer is the biggest of all Co layers, the contributions from the first Pt layer and from the first vacuum layer reduce the total difference conductivity. From the lower parts in Figs. 5 - 7 one easily can follow the various layer-wise contributions to the total difference conductivity when the orientation in the sample subsystem gradually changes from perpendicular to in-plane.

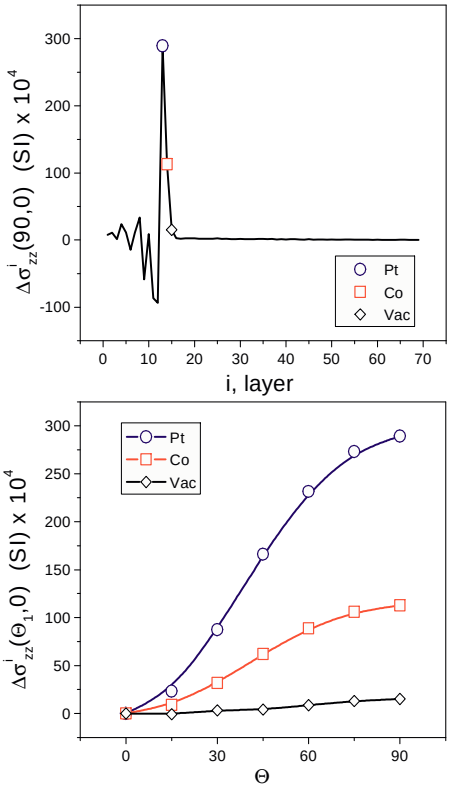

FIG. 5: (color online) Top: Layer-wise contributions to the total difference conductivity for a single monolayer of Co on top of Pt(111). Bottom: Peak values as indicated explicitly. $\Theta_1^{(r)}, \Theta_2^{(r)} = 0$.

Time scales

Since the derivative of the free energy with respect to the orientation of the magnetization is nothing but the internal field in the Landau-Lifshitz-Gilbert equation [34–37], e.g., the times $\tau(\Theta, 0)$ needed to move along a particular path $\Delta E(\Theta, 0)$, $\Theta_1^{(r)}, \Theta_2^{(r)} = 0$, from $\Theta = 0$ to a particular value of Θ on the free energy hypersurface, can easily be evaluated [43] by considering only the precessional term in this equation.[38] In the top two entries of Fig. 8 such switching times are displayed for $n \leq 3$ as a function of Θ together with the switching time $\tau(0, \Theta)$ corresponding to $\Delta E(0, \Theta), 0 \leq \Theta \leq 90$ for $n = 1$. It is interesting to note that the actual switching time is

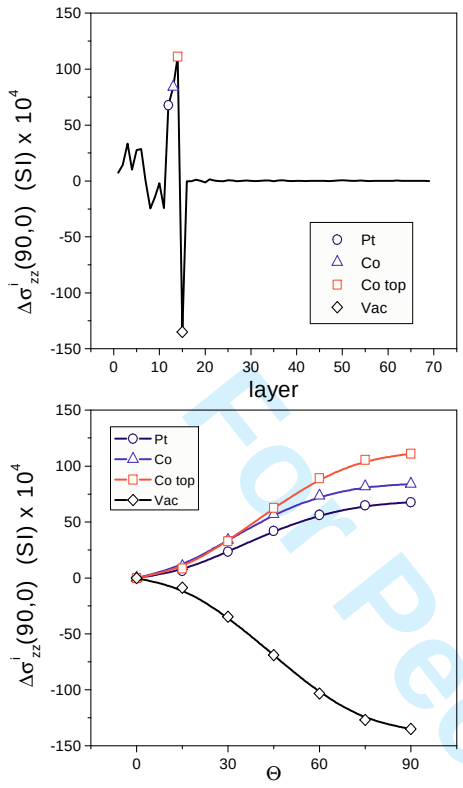

FIG. 6: (color online) Top: Layer-wise contributions to the total difference conductivity for a two monolayers of Co on top of Pt(111). Bottom: Peak values as indicated explicitly. $\Theta_1^{(r)}, \Theta_2^{(r)} = 0$.

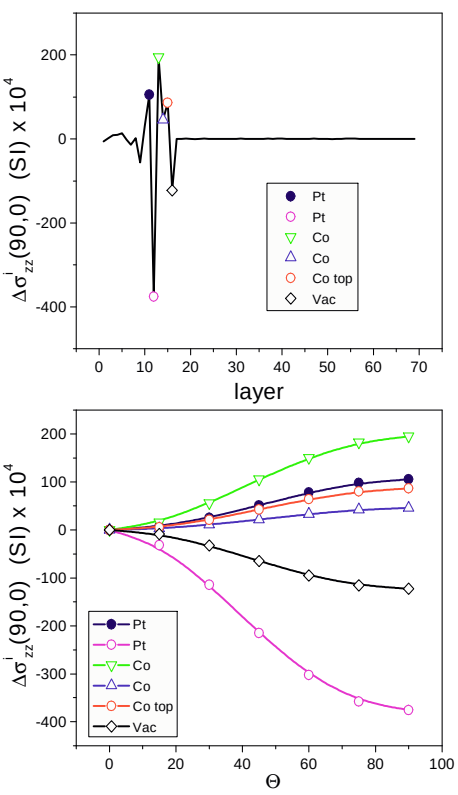

FIG. 7: (color online) Top: Layer-wise contributions to the total difference conductivity for a three monolayers of Co on top of Pt(111). Bottom: Peak values as indicated explicitly. $\Theta_1^{(r)}, \Theta_2^{(r)} = 0$.

mostly determined by the time needed to leave the equilibrium position (lowest free energy). Quite obviously to switch for $n = 1$ from perpendicular to in-plane is quite a bit slower than to switch for $n > 1$ from in-plane to perpendicular. In the case of a single layer of Co on Pt(111) $\tau(\Theta, 0) \gg \tau(0, \Theta)$, only for two layers of Co the two switching times are about the same, $\tau(\Theta, 0) \sim \tau(0, \Theta)$.

In Fig. 8 finally the total difference conductivities viewing only the sample subsystem, $\Delta\sigma_{zz}(\Theta, 0)$, for Pt(111)/$Co_n$, $n \leq 3$, are displayed versus Θ and as implicit functions of the corresponding free energy $\Delta E(\Theta, 0)$. The reason that in the upper part of Fig. 8 there is a maximum around $\Theta = 45$ for $n = 3$ can easily be understood from Fig. 7: for $\Theta > 45$ the contribution from the first Pt layer grows much faster than all other contributions. Also displayed is $\Delta\sigma_{zz}(0, \Theta)$ versus Θ in the case of $n = 1$.

If $\tau(0, \Theta) \ll \tau(\Theta, 0)$, as is the case for $n = 1$, then in Eq. (9) most likely the reference configuration for free energies $\Delta E > \Delta E(90, 0)$ is $\Theta_1^{(r)} = 90$, $\Theta_2^{(r)} = 0$, i.e., a corresponding difference conductivity, $\Delta\sigma_{zz}(\Theta_1, \Theta_2) = \sigma_{zz}(90, \Theta_2) - \sigma_{zz}(90, 0)$, has to be viewed with respect to the point at which the reorientation transition for sample part of the system is reached ($\Delta E(90, \Theta) = \Delta E(90, 0) + \Delta E(0, \Theta)$). This particular case is displayed in the lower part of Fig. 9 using a dashed line. It should be noted that because for the evaluation of the free energies $E(\Theta_1, 0)$ the reference configuration was the perpendicular arrangement ($\Theta_1^{(r)}, \Theta_2^{(r)} = 0$), in Fig. 9 the absolute value of the free energy is taken as argument.

The theoretical spectra

The lower part of Fig. 9 is now the ultimate result of the present investigations. The curves shown correspond to the positive magnetic field part of an experimental di/dV spectrum when varying the external magnetic field. In fact, the curve for $n = 1$ looks very similar in shape to that in the experimental [2] and theoretical spectrum [15, 16] of Co_2/Cu(111): a sharp drop in the difference conductivity exactly at the reorientation energy is "seen".

Quite clearly by taking for example again the case for

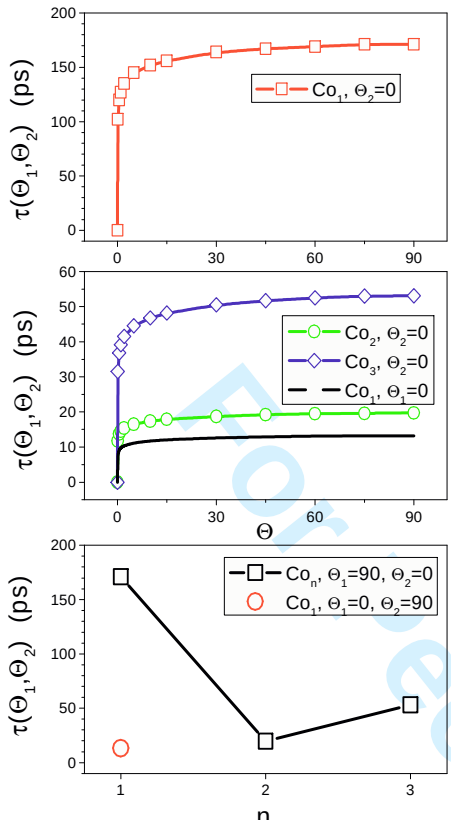

FIG. 8: Switching times for $n \leq 3$ monolayers of (color online) Co on top of Pt(111). Top: $n = 1$, switching from perpendicular to in-plane, middle: $n > 1$, switching from in-plane to perpendicular. Bottom: comparison of the switching times to reach the reorientation transition with respect to the number of Co layers.

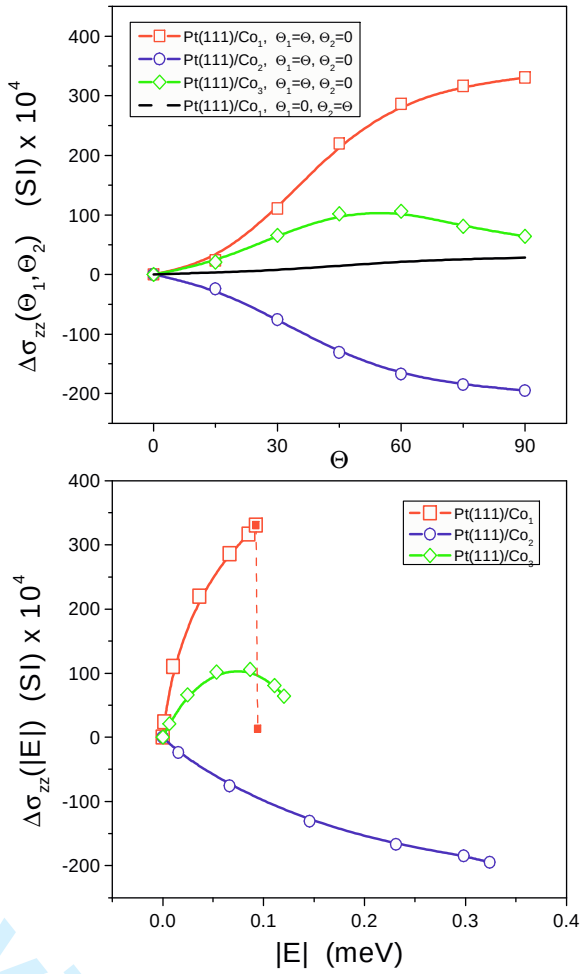

FIG. 9: (color online) Top: Difference conductivity $\Delta\sigma_{zz}(\Theta_1.\Theta_2)$ for $n \leq 3$ monolayers of Co on top of Pt(111). For $n = 1$ also difference conductivity corresponding to the tip part of the system is displayed. Bottom: difference conductivity for for $n \leq 3$ monolayers of Co on top of Pt(111) as an implicit function of the corresponding free energy.

$n = 1$ the theoretical (and so also the experimental) spectrum – a single curve – yields of course no indication whatsoever why there is an abrupt change at a particular strength of the external field or what causes the gradual rise in the difference conductivity up to this strength. In order to interpret the two branches of that curve additional concepts are needed such as arguments based on the dynamics of the system during a reorientation of the magnetization. Furthermore, the differences between one, two and three layers of Co on top of Pt(111) can easily be explained in terms of the different reorientation energies. Finally, at least a qualitative description of what is actually "seen" in experiment – the claim of atom-specific resolution in contrast – can be given in terms of layer-wise contributions to the total difference conductivities.

CONCLUSION

It was shown that for very large systems consisting of two subsystems separated by a vacuum barrier a stacking together of the subsystems can approximately be used. By displaying $\Delta\sigma_{zz}(\Theta_1, \Theta_2)$ versus $\Delta E(\Theta_1, \Theta_2)$, which is proportional to the applied external magnetic field, a quantity is found that directly corresponds to experimental di/dV curves as the external magnetic field is varied. Furthermore, it turned out that for Pt(111)/Co$_n$, $n \leq 3$, quite different situations seem to be present as far as the corresponding reorientation energies and the main contributions to the total difference conductivity $\Delta\sigma_{zz}(\Theta_1, \Theta_2)$ are concerned.

[1] R. Wiesendanger, Rev. of Mod. Phys. **81**, 1495 (2009).
[2] G. Rodary, S. Wedekind, D. Sander, and J. Kirschner, Jpn. J. Appl. Phys. **47**, 9013 (2008).
[3] T. Balashov, T. Schuh, A. F. Takács, E. Ernst, S. Ostanin, J. Henk, I. Mertig, P. Bruno, T. Miyamachi, S. Suga, and W. Wulfhekel, Phys. Rev. Lett. **102**, 257203 (2009).
[4] F. Meier, L. Zhou, J. Wiebe, and R. Wiesendanger, Science **320**, 82 (2008).
[5] F. Meier, K. von Bergmann, J. Wiebe, M. Bode, and R. Wiesendanger, Appl. Phys. **40**, 1306 (2007).
[6] J. Bardeen, Phys. Rev. Lett. **6**, 57 (1961).
[7] J. Tersoff and D. R. Hamann, Phys. Rev. Lett. **50**,1998 (1983).
[8] J. Tersoff and D. R. Hamann, Phys. Rev. B **31,** 805 (1985).
[9] D. Drakova, Rep. Prog. Phys. **64**, 205 (2001); J. M. Blanco, F. Flores, Rubén Pérez, Progr. Surf. Sci. **81**, 403 (2006).
[10] O. O. Brovko, V. S. Stepanyuk, W. Hegert, and P. Bruno, Phys. Rev. B **79**, 245417 (2009).
[11] Kun Tao, V. S. Stepanyuk, W. Hegert, I. Rungger, S. Sanvito, and P. Bruno, Phys. Rev. Lett. **103**, 057202 (2009).
[12] X.-D. Ma, D. I. Bazhanov, O. Fruchart, F. Yildiz, T. Yokoyama, M. Przybylski, V. S. Stepanyuk, W. Hegert, and J. Kirschner, Phys. Rev. Lett. **102**, 205503 (2009).
[13] M. Bode, S. Heinze, A. Kubetzka, O. Pietzsch, X. Nie, G. Bihlmayer, S. Blügel, and R. Wiesendanger, Phys. Rev. Lett. **89**, 237205 (2002).
[14] C. Li, A. J. Freeman, H. J. F. Jansen, and C. L. Fu, Phys. Rev. B **42**, 5433 (1990).
[15] P. Weinberger, Phys. Rev. B **80**, 060403 (2009).
[16] P. Weinberger, Phys. Rev. B **81**, 174410 (2010).
[17] C. Blaas, P. Weinberger, L. Szunyogh, P.M. Levy and C. Sommers, Phys. Rev. B **60**, 492 (1999).
[18] P. Weinberger, *Magnetic Anisotropies in Nanostructured Matter* (CRC Boca Raton London New York, 2008).
[19] J. Zabloudil, R. Hammerling, L. Szunyogh and P. Weinberger, *Electron Scattering in Solid Matter* (Springer Berlin Heidelberg New York, 2004).
[20] K. Palotas, B. Lazarovits, L. Szunyogh, and P. Weinberger, Phys. Rev. B **70**, 134421 (2004).
[21] A. Vernes, B. L. Gyorffy, and P. Weinberger, Phys. Rev. B **76**, 012408 (2007)
[22] B. Újfalussy, B. Lazarovits, L. Szunyogh, G. M. Stocks, and P. Weinberger, Phys. Rev. B **70**, 100404(R)/1-4 (2004).
[23] C. Etz, J. Zabloudil, P. Weinberger, and E. Y. Vedmedenko, Phys. Rev. B **77**, 184425 (2008).
[24] P. Weinberger, A. Vernes, L. Szunyogh, and J. Zabloudil, Phys. Rev. B **80**, 075430 (2009).
[25] It should be noted that in a similar formal manner, e.g., s-, p-, and d-like densities-of-states are introduced as angular momentum projected contributions to the density of states.
[26] R. Kubo, M. Toda, N. Hashitsume, *Statistical physics II: Non-equilibrium Statistical Mechanics*, Springer, Berlin (1985); R. Kubo, J. Phys. Soc. Jpn. **12**, 570 (1957).
[27] J. M. Luttinger, in *Mathematical Methods in Solid State and Superfluid Theory* (Oliver and Boyd, Edinburgh) Chap. 4, pp. 157 (1962).
[28] D. A. Greenwood, Proc. Phys. Soc. London **71**, 585 (1958).
[29] W. H. Butler, Phys. Rev. B **31**, 3260 (1985).
[30] P. M. Levy, Solid State Physics Vol. 47, eds. H. Ehrenreich and D. Turnbull (Academic Press, Cambridge, MA, 1994) pp. 367-462.
[31] H. E. Camblong, P. M. Levy, and S. Zhang, Phys. Rev. B **51**, 16052 (1995).
[32] P. M. Levy and I. Mertig, In: *Spin-dependent transport in Magnetic Nanostructures*, Eds. T. Shinjo and S. Maekawa, Gordon and Breach Science Publisher (2001).
[33] P. Weinberger, Physics Reports **377**, 281 (2003).
[34] L. D. Landau and E. M. Lifshitz, *Statistical Physics*, Vol. 9 of *Course of Theoretical Physics* (Pergamon Press, Oxford, 1999).
[35] J. C. Mallinson, IEEE Transactions on Magnetics **36**, 1976 (2000).
[36] B. Heinrich, R. Urban, and G. Woltersdorf, IEEE Transactions on Magnetics **38**, 2496 (2002).
[37] J. Kunes and V. Kambersky, Phys. Rev. B **65**, 212411 (2002).
[38] P. Weinberger, A. Vernes, B. L. Gyorffy, and L. Szunyogh, Phys. Rev. B **70**, 094401 (2004).
[39] S. H. Vosko, L. Wilk, and M. Nusair, Can. J. Phys. **58**, 1200 (1980).
[40] P. Weinberger, Phys. Rev. B **81**, 184412 (2010).
[41] K. Palotas, B. Lazarovits, L. Szunyogh, and P. Weinberger, Phys. Rev. B **67**, 174404 (2003).
[42] In a real space formulation of the Kubo equation [20] this implies that atom- or site-specific contributions to the contrast can be evaluated.
[43] Since very little is known about the actual values of the so-calling damping parameter α in nano-sized systems, in here α was set to unity.

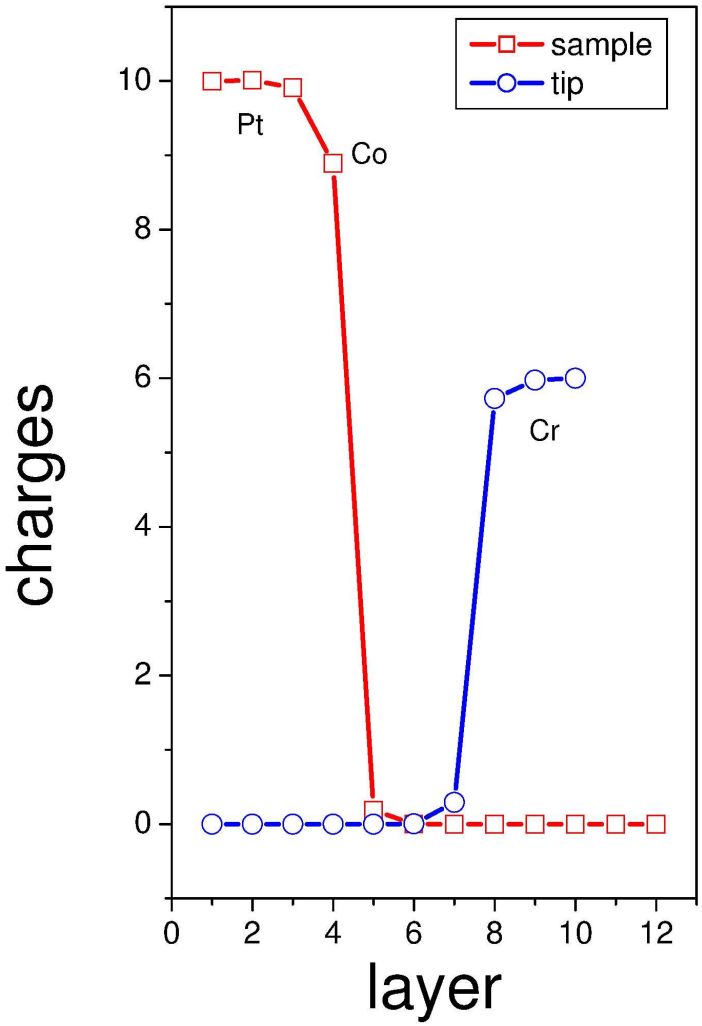

Free energy $E(\Theta_1, \Theta_2)$, $\Theta_1 ^{(r)}, \Theta_2 ^{(r)}=0$, corresponding to n≤3 monolayers of Co on top of Pt(111). In the case of a single monolayer of Co also the free energy corresponding to the tip part of the system is displayed.
209x297mm (600 x 600 DPI)

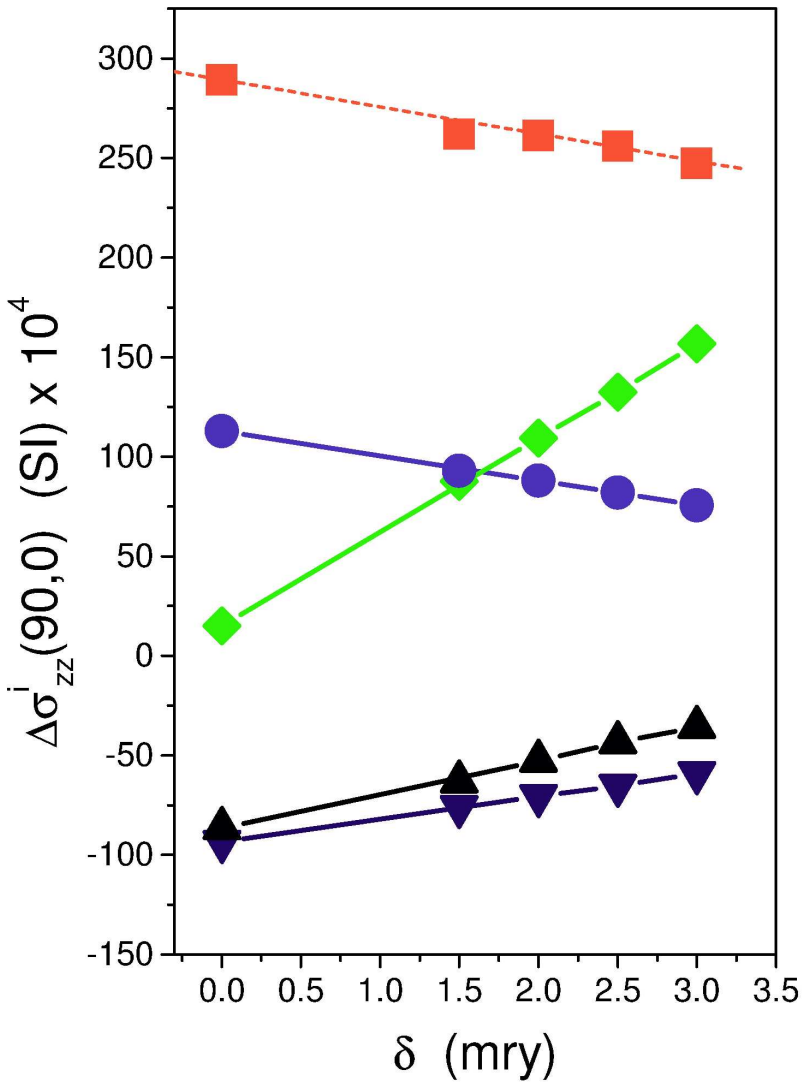

Numerical continuation of local difference conductivities Δσ_{zz}^{i}(Θ□,0), Θ□=90, Θ□^{(r)},Θ□^{(r)}=0, see Eq. (<ref>e-8</ref>), to the real axis for Pt(111) covered by a single layer of Co. Diamonds denote the Co layer, squares, up- and down triangles in turn the first, second and third Pt layer beneath, circles refer to the first vacuum layer ("surface state").
215x279mm (600 x 600 DPI)

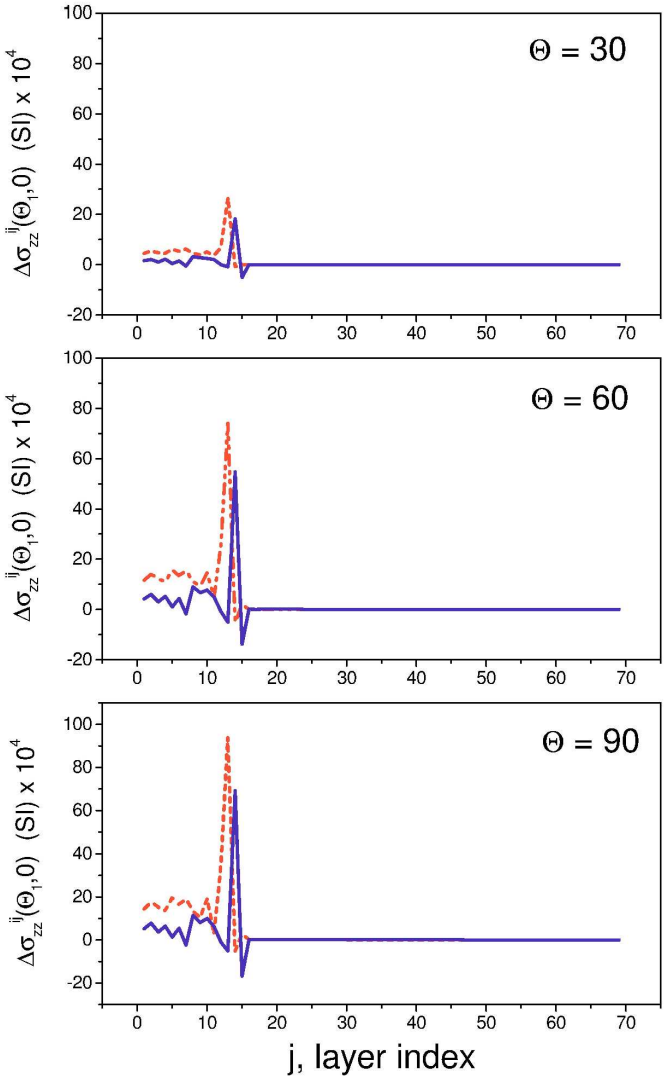

Evaluation of peaks in the layer-wise difference conductivities Δσ_{zz}^{ij}(Θ,0), Θ_1^{(r)},Θ_2^{(r)}=0, for Pt(111)/Co when varying Θ between 0 and 90. Note that Δσ_{zz}^{ij}(0,0) is of course zero for all i and j. The full line applies when i refers to the Co layer, the dashed line to the Pt layer beneath.
215x279mm (600 x 600 DPI)

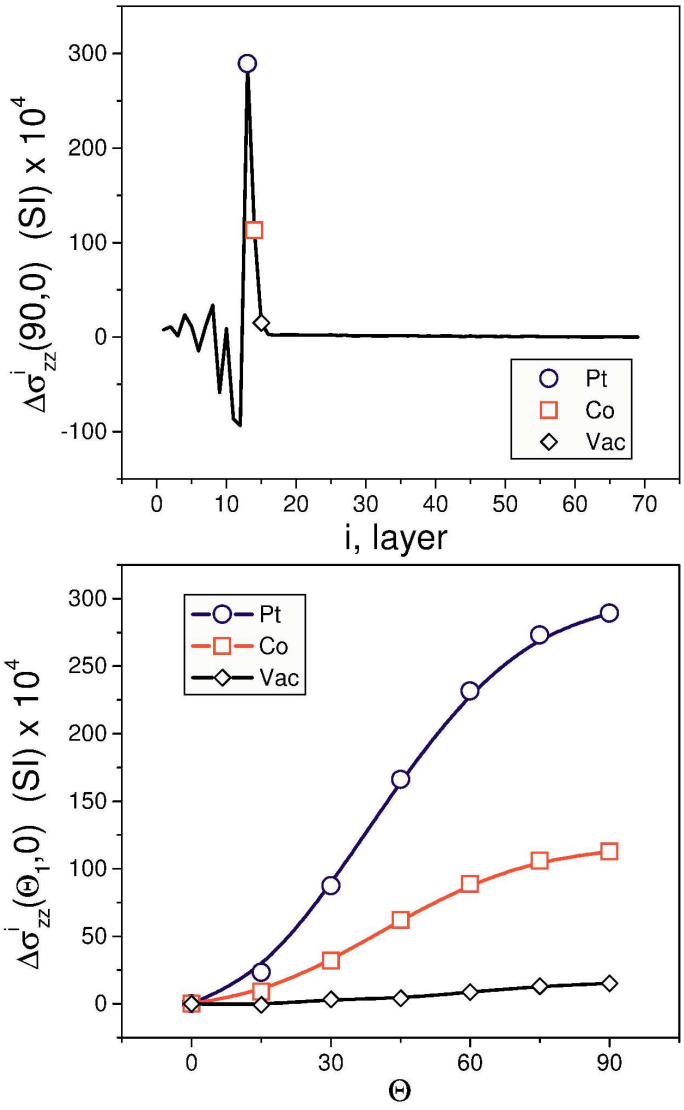

Top: Local difference conductivities for a single monolayer of Co on top of Pt(111). Bottom: Peak values as indicated explicitly. Θ₁^{(r)},Θ₂^{(r)}=0.
215x279mm (600 x 600 DPI)

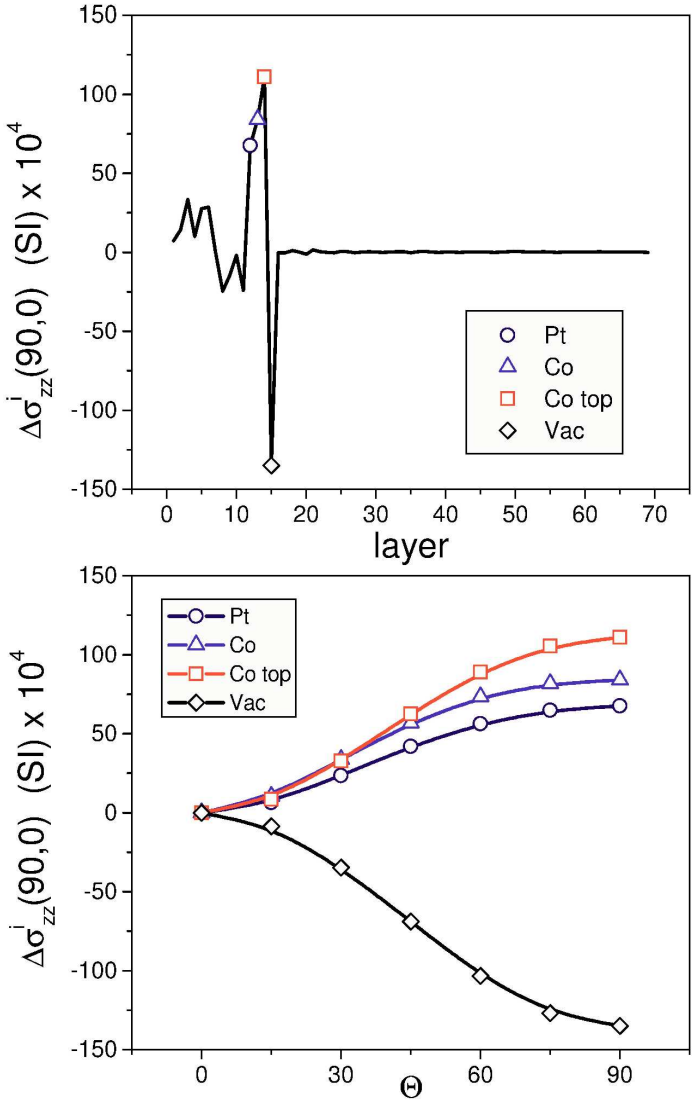

Top: Local difference conductivities for a two monolayers of Co on top of Pt(111). Bottom: Peak values as indicated explicitly. Θ₁^{(r)},Θ₂^{(r)}=0.
215x279mm (600 x 600 DPI)

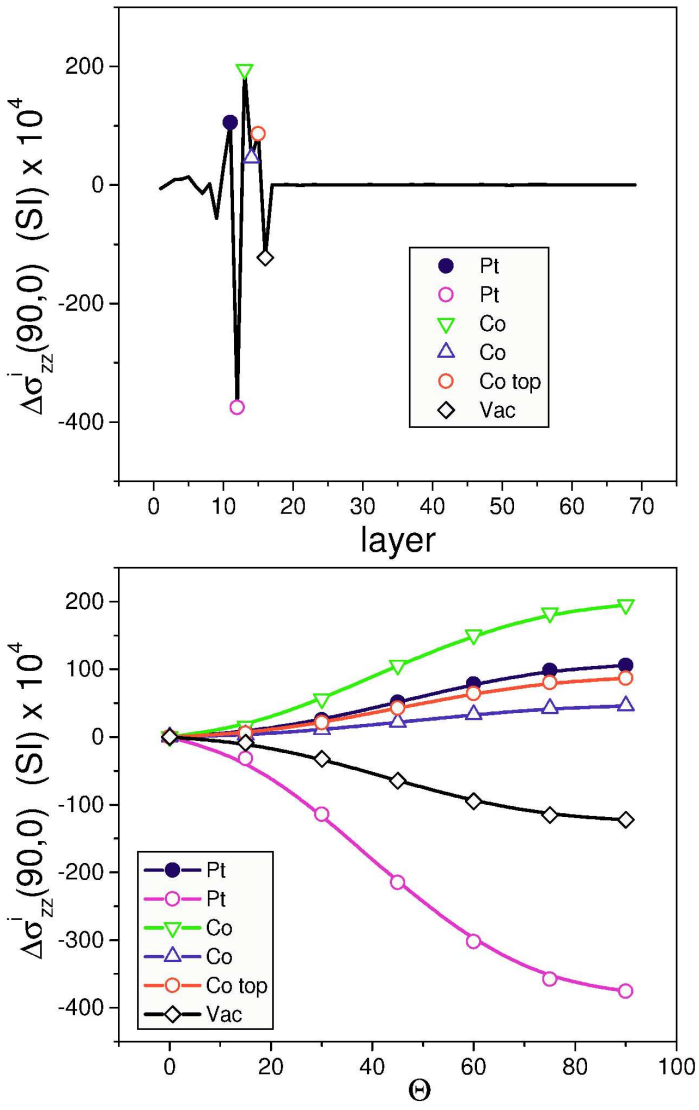

Top: Local difference conductivities for a three monolayers of Co on top of Pt(111). Bottom: Peak values as indicated explicitly. Θ₁^{(r)},Θ₂^{(r)}=0.
215x279mm (600 x 600 DPI)

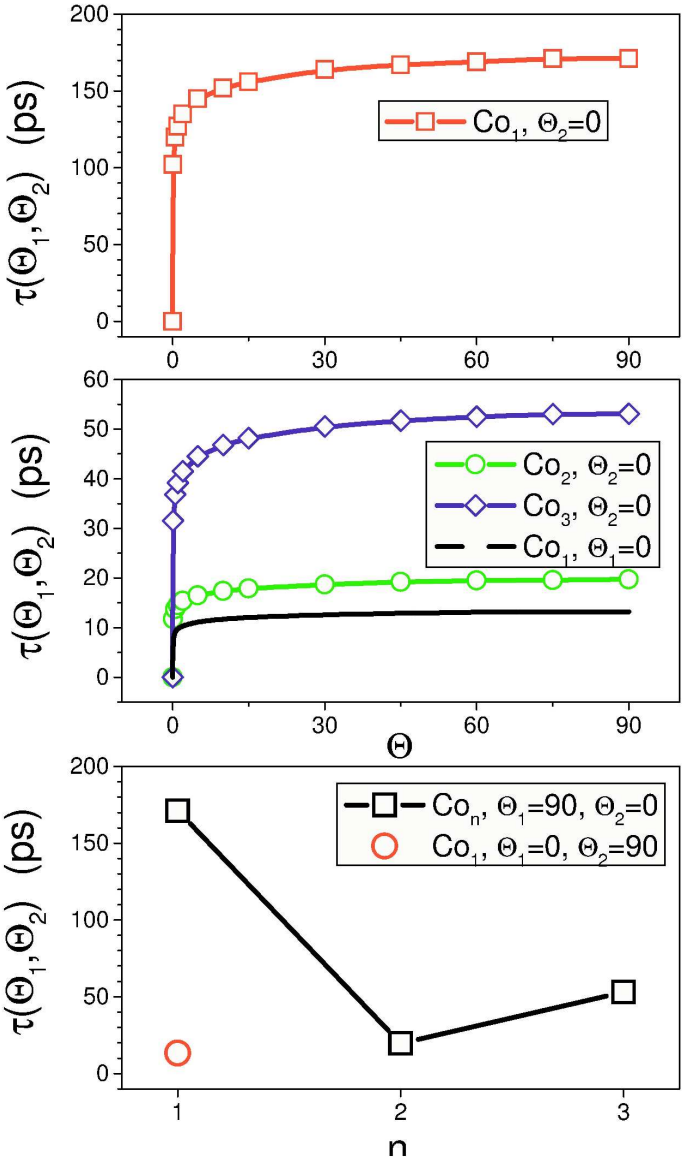

Co on top of Pt(111). Top: n=1, switching from perpendicular to in-plane, middle: n>1, switching from in-plane to perpendicular. Bottom: comparison of the switching times to reach the reorientation transition with respect to the number of Co layers.
215x279mm (600 x 600 DPI)

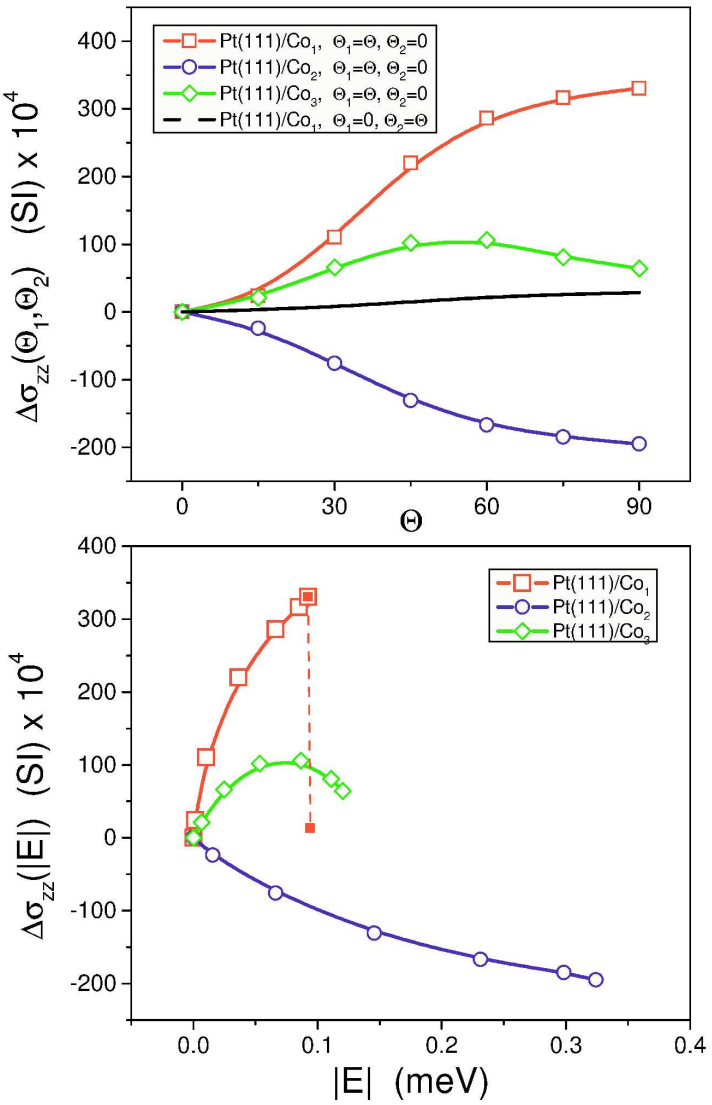

Top: Difference conductivity Δσ_{zz}(Θ₁.Θ₂) for n≤3 monolayers of Co on top of Pt(111). For n=1 also difference conductivity corresponding to the tip part of the system is displayed. Bottom: difference conductivity for for n≤3 monolayers of Co on top of Pt(111) as an implicit function of the corresponding free energy.
215x279mm (600 x 600 DPI)

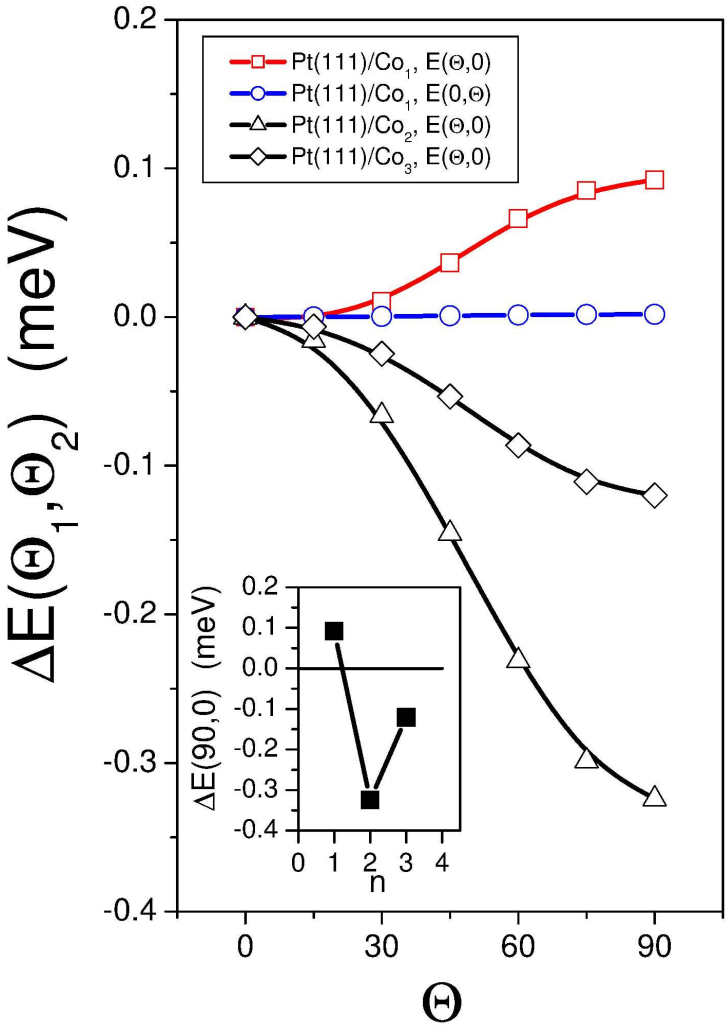

Free energy ΔE(Θ₁,Θ₂), Θ₁^{(r)},Θ₂^{(r)}=0, corresponding to n≤3 monolayers of Co on top of Pt(111). In the case of a single monolayer of Co also the free energy corresponding to the tip part of the system is displayed. The inset shows the reorientation (from perpendicular to in-plane) energy as a function of n.
209x297mm (600 x 600 DPI)